A Numerical Convergence Study of some Open Boundary Conditions for Euler equations

Clément Colas, Martin Ferrand, Jean-Marc Hérard, Olivier Hurisse, Erwan Le Coupanec, Lucie Quibel

▶ **To cite this version:**

Clément Colas, Martin Ferrand, Jean-Marc Hérard, Olivier Hurisse, Erwan Le Coupanec, et al.. A Numerical Convergence Study of some Open Boundary Conditions for Euler equations. 2019. hal-02422802v1

HAL Id: hal-02422802

https://hal.science/hal-02422802v1

Preprint submitted on 23 Dec 2019 (v1), last revised 28 Jan 2020 (v2)

HAL is a multi-disciplinary open access archive for the deposit and dissemination of scientific research documents, whether they are published or not. The documents may come from teaching and research institutions in France or abroad, or from public or private research centers.

L'archive ouverte pluridisciplinaire **HAL**, est destinée au dépôt et à la diffusion de documents scientifiques de niveau recherche, publiés ou non, émanant des établissements d'enseignement et de recherche français ou étrangers, des laboratoires publics ou privés.

A Numerical Convergence Study of some Open Boundary Conditions for Euler equations

Clément Colas, Martin Ferrand, Jean-Marc Hérard, Olivier Hurisse, Erwan Le Coupanec and Lucie Quibel

Abstract We discuss herein the suitability of some open boundary conditions while comparing approximate solutions of one-dimensional Riemann problems in a bounded sub-domain with the restriction in this sub-domain of the exact solution in the infinite domain, considering the Euler system of gas dynamics. Assuming that no information is known from outside of the domain, some basic open boundary condition specifications are given, and a measure of the L^1 norm of the error inside the computational domain enables to show consistency errors in situations involving outgoing shock waves, depending on the chosen boundary condition formulation. This investigation has been performed with Finite Volume methods, using approximate Riemann solvers in order to compute numerical fluxes for both inner and boundary interfaces.

Key words: Finite volumes, approximate Riemann solver, open boundary conditions, Euler equations, compressible flow

MSC (2010)**:** 65M08, 65N08, 76N15

C. Colas[1,2] · M. Ferrand[1,3] · J.-M. Hérard[1,2] · O. Hurisse[1] · E. Le Coupanec[1] · L. Quibel[1,4]
[1]EDF R&D, MFEE, 6 quai Watier, 78400, Chatou, France
[2]Aix-Marseille Université, I2M, UMR CNRS 7373, 39 rue Joliot Curie, 13453, Marseille, France
[3] CEREA Lab (Ecole des Ponts ParisTech - EDF R&D), 6-8 avenue Blaise Pascal, Cité Descartes, 77420 Champs-sur-Marne, France
[4] Université de Strasbourg, IRMA, UMR CNRS 7501, 7 rue René Descartes, 67084, Strasbourg, France
e-mail: clement.colas@edf.fr, martin.ferrand@edf.fr, jean-marc.herard@edf.fr, olivier.hurisse@edf.fr, erwan.lecoupanec@edf.fr, lucie.quibel@edf.fr

1 Introduction

Concerning computational fluid dynamics, industrial simulations are frequently performed with a partial or total unknown fluid state outside of the computational domain. How are boundary conditions dealt with when no information is known outside? Here the one-dimensional Euler equations governing inviscid compressible fluid flows are considered. The unknowns ρ, u, P respectively denote the density, the velocity and the pressure of the fluid, while the momentum is $Q = \rho u$. The total energy E is such that $E = \rho\left(\frac{u^2}{2} + \varepsilon\right)$. The internal energy $\varepsilon(P,\rho)$ is prescribed by the EOS (Equation Of State). In the sequel, we note $\boldsymbol{W} = (\rho, Q, E)^t$ the conservative variable, $\boldsymbol{Y} = (s, u, P)^t$ the non-conservative variable, with s the entropy, and $\boldsymbol{F}(\boldsymbol{W}) = (Q, Qu + P, (E+P)u)^t$ the flux function, so that the set of governing equations reads:

$$\partial_t \boldsymbol{W} + \partial_x \boldsymbol{F}(\boldsymbol{W}) = 0\,. \tag{1}$$

The speed of sound noted c is such that $c^2 = \left(\frac{P}{\rho^2} - \frac{\partial\varepsilon(P,\rho)}{\partial\rho}\right) / \left(\frac{\partial\varepsilon(P,\rho)}{\partial P}\right)$.

One pioneering work on boundary conditions for bounded domain may be found in [1]. Actually, the present work addresses the issue of open numerical boundary conditions to get waves outside of the computational domain and can be connected to the work of [6]. The solution of Euler system (1) is sought in $\mathbb{R}\times(0,T)$, with time $T \in \mathbb{R}_+^*$, without boundary conditions, see [10]. This solution, expected to be known and unique, is noted $\boldsymbol{W}_{\Omega_\infty}^{exact}(x,t)$ for $(x,t) \in \mathbb{R}\times(0,T)$.

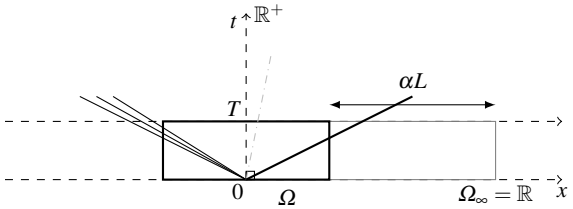

Fig. 1 Bounded computational domain $\Omega \subsetneq \Omega_\infty$, with Ω_∞ a spatial infinite domain.

In contrast, the numerical approximations, noted $\boldsymbol{W}_{\Omega}^{\Delta x,\Delta t}(x,t)$ for $(x,t) \in \Omega \times (0,T)$, are performed in a bounded computational sub-domain $\Omega \subsetneq \Omega_\infty$ (see Fig. 1) with prescribed open inlet/outlet boundary conditions on $\partial\Omega$.

For this purpose, artificial boundaries are introduced on $\partial\Omega$. Then, numerical boundary conditions, depending on the time and space steps, must be prescribed on $\partial\Omega$. When $(\Delta x, \Delta t) \to (0,0)$, we assume that some (unique) converged approximation, noted $\boldsymbol{W}_{\Omega}^{0,0}(x,t)$ for $(x,t) \in \Omega \times (0,T)$, is obtained. Eventually, we wonder whether $\boldsymbol{W}_{\Omega}^{0,0}(x,t)$ for $(x,t) \in \Omega \times (0,T)$, coincides with the restriction of the ex-

act solution to Ω, $\boldsymbol{W}_{\Omega_\infty}^{exact}(x,t)$ for $(x,t) \in \Omega \times (0,T)$, or not. In the latter case, the converged approximation $\boldsymbol{W}_{\Omega}^{0,0}$ will be said to be **non-consistent**.

For Euler system (1), a measure of a subsonic state in the last inner cell N (eigenvalues $\lambda_1(\mathbf{W}_N^n) < 0$ and $\lambda_{2,3}(\mathbf{W}_N^n) > 0$) at a right outlet will require one scalar external information, whereas in the supersonic case ($\lambda_{1,2,3}(\mathbf{W}_N^n) > 0$), the upwind state will be privileged. Actually, we recall that in the subsonic case, the approach of [4, 5] may provide some way to cope with the lack of information.

A first drawback of the latter approach is that the sign of eigenvalues may easily change: signs of eigenvalues $\lambda_k(\mathbf{W}_N^n)$ are not necessarily representative of what happens really at the right boundary when computing true waves associated with the 1D Riemann problem with the initial condition: $\boldsymbol{W}_L = \mathbf{W}_N^n$ and $\boldsymbol{W}_R = \mathbf{W}_{ext}^n$ (unless when $\mathbf{W}_{ext}^n = \mathbf{W}_N^n$). A very instructive example is given in [6] Sect. 3.2, while restricting on a scalar problem (Burger equation). A second question is: assuming that nothing is known about the exterior state $\mathbf{W}_{ext}^n$, how does the solution, inside the computational sub-domain, depend on the choice of $\mathbf{W}_{ext}^n$?

Herein, the aim consists in testing suitable numerical boundary conditions in the sense that they converge towards the exact, not necessarily regular, solution.

2 Finite volume method

We briefly recall the basis of the explicit finite volume scheme VFRoe-ncv, an approximate Godunov scheme using non conservative variables [8, 7]. For the sake of simplicity, regular meshes of the one-dimensional computational domain are considered of size $\Delta x = x_{i+1/2} - x_{i-1/2}$, $i \in \{1,...,N\}$, and $\Delta t^n = t^{n+1} - t^n$ is the time step, $n \in \mathbb{N}$. The time step is given by some CFL condition in order to gain stability. Let $\mathbf{W}_i^n$ be an approximation of the mean value $\dfrac{1}{\Delta x}\displaystyle\int_{x_{i-1/2}}^{x_{i+1/2}} \mathbf{W}(x,t^n)dx$. Time-space integration of system (1) over $\left[x_{i-1/2}, x_{i+1/2}\right] \times \left[t^n, t^{n+1}\right]$ provides the standard following scheme:

$$\Delta x(\mathbf{W}_i^{n+1} - \mathbf{W}_i^n) + \Delta t^n \left(\mathbf{g}_{i+\frac{1}{2}}^n - \mathbf{g}_{i-\frac{1}{2}}^n\right) = 0\,, \tag{2}$$

where $\mathbf{g}_{i+1/2}^n$ is the numerical flux through the interface $\left\{x_{i+1/2}\right\} \times \left[t^n, t^{n+1}\right]$. For so-called first-order space scheme, $\mathbf{g}_{i+1/2}^n = \mathbf{g}(\mathbf{W}_i^n, \mathbf{W}_{i+1}^n)$. The numerical flux $\mathbf{g}_{i+1/2}^n$ is obtained by solving the linearized Riemann problem:

$$\begin{cases} \partial_t \boldsymbol{Y} + \boldsymbol{B}(\widetilde{\boldsymbol{Y}})\partial_x \boldsymbol{Y} = 0\,, \\ \boldsymbol{Y}(\boldsymbol{x}, t^n) = \begin{cases} \mathbf{Y}_i^n & \text{if } x < x_{i+\frac{1}{2}}\,, \\ \mathbf{Y}_{i+1}^n & \text{if } x > x_{i+\frac{1}{2}}\,, \end{cases} \end{cases} \tag{3}$$

where $\widetilde{\boldsymbol{Y}} = (\mathbf{Y}_i^n + \mathbf{Y}_{i+1}^n)/2$ and $\boldsymbol{B}(\boldsymbol{Y})$ stands for the following matrix:

$$\boldsymbol{B}(\boldsymbol{Y}) = (\partial_{\boldsymbol{Y}}\boldsymbol{W})^{-1}\,\partial_{\boldsymbol{W}}\boldsymbol{F}(\boldsymbol{W})\partial_{\boldsymbol{Y}}\boldsymbol{W}\ .$$

Once the exact solution $\boldsymbol{Y}^\star\left(\frac{x-x_{i+1/2}}{t};\mathbf{Y}_i^n,\mathbf{Y}_{i+1}^n\right)$ of problem (3) is computed, the numerical flux is defined as:

$$\mathbf{g}_{i+\frac{1}{2}}^n = \mathbf{g}(\mathbf{W}_i^n,\mathbf{W}_{i+1}^n) = \boldsymbol{F}(\boldsymbol{W}(\boldsymbol{Y}^\star(0;\mathbf{Y}_i^n,\mathbf{Y}_{i+1}^n))\ . \tag{4}$$

This numerical flux will be used for both inner interfaces and boundary interfaces.

3 Numerical boundary conditions for outgoing waves

We propose numerical artificial boundary conditions when no information is given on the open boundary of the computational sub-domain. One possible approach is to determine an artificial state $\mathbf{W}_{ext}^n$ in the virtual cell, symmetric of the boundary cell $\mathbf{W}_i^n$, outside of the sub-domain. The numerical boundary flux is then obtained by $\mathbf{g}_{1/2}^n = \mathbf{g}(\mathbf{W}_{ext,1}^n,\mathbf{W}_1^n)$ and $\mathbf{g}_{N+1/2}^n = \mathbf{g}(\mathbf{W}_N^n,\mathbf{W}_{ext,N}^n)$.

Outgoing rarefaction wave

a. Formulation assuming the invariance of the interior state BC_0

The first boundary condition, widely used in industrial simulations, simply consists in taking the interior state $\mathbf{W}_i^n$ of the boundary cell at each time step t^n

$$\mathbf{W}_{ext}^n = \mathbf{W}_N^n\ . \tag{5}$$

The numerical boundary flux thus reads $\mathbf{g}_{N+1/2}^n = \mathbf{g}(\mathbf{W}_N^n,\mathbf{W}_N^n) = \boldsymbol{F}(\mathbf{W}_N^n)$. This technique does not need any knowledge about the wave structure.

b. Formulation using the wave structure and an extrapolation of the interior state BC_r

The second boundary condition is built by using the two associated Riemann invariants of the regular wave and a third additional scalar relation. Note that, for an ideal gas, the exact velocity profile is linear w.r.t. x at time t^n. Thus, for an ideal gas EOS such that $\rho\varepsilon = P/(\gamma-1)$, with $\gamma > 1$, we get:

$$\rho_{ext}^n = \rho_N^n\left(1-\frac{\gamma-1}{2}\frac{u_{N-1}^n-u_N^n}{c_N^n}\right)^{\frac{2}{\gamma-1}},\ P_{ext}^n = P_N^n\left(1-\frac{\gamma-1}{2}\frac{u_{N-1}^n-u_N^n}{c_N^n}\right)^{\frac{2\gamma}{\gamma-1}}$$

and $u_{ext}^n = 2u_N^n - u_{N-1}^n$. The numerical boundary flux is computed as following $\mathbf{g}_{N+1/2}^n = \mathbf{g}(\mathbf{W}_N^n,\mathbf{W}_{ext}^n)$. This technique connects the interior state with the exterior virtual state by using the rarefaction wave structure.

Outgoing shock wave

a. Formulation assuming the invariance of the interior state BC_0

Same as for rarefaction wave.

c. Formulation using the far-field state BC_s

The boundary interior cell N is connected with the right initial state $\boldsymbol{W}_R^0$ by a virtual exterior cell of physical size αL, with L the domain length and $\alpha \in \mathbb{R}_+^*$ a parameter, see Fig. 1. Inspired by [3], this exterior state $\mathbf{W}_{ext}^n$ is updated with the numerical flux and the known state $\boldsymbol{W}_R^0$ such that:

$$\alpha L \left(\mathbf{W}_{ext}^n - \mathbf{W}_{ext}^{n-1}\right) + \Delta t^{n-1} \left(\mathbf{g}(\mathbf{W}_{ext}^{n-1}, \mathbf{W}_R^0) - \mathbf{g}(\mathbf{W}_N^{n-1}, \mathbf{W}_{ext}^{n-1})\right) = 0\,. \qquad (6)$$

This technique gives the following asymptotic update of the exterior state $\mathbf{W}_{ext}^n$ when $\alpha \to +\infty$ for a finite time step Δt^{n-1}: $\lim_{\alpha\to+\infty} \mathbf{W}_{ext}^n = \mathbf{W}_{ext}^{n-1}$. The exterior state is steady and therefore equal to its initial state $\mathbf{W}_{ext}^0$, which is the right state $\boldsymbol{W}_R^0$. The numerical boundary flux thus yields: $\mathbf{g}_{N+1/2}^n = \mathbf{g}(\mathbf{W}_N^n, \mathbf{W}_R^0)$. This asymptotic boundary condition amounts to impose, in the virtual exterior cell, the right state $\boldsymbol{W}_R^0$ known from the initial condition of the Cauchy problem.

4 Numerical results

We discuss below some results of this preliminary study. Other results with distinct EOS are available in [2]. Two subsonic test cases, corresponding to 1D Riemann problems with a diatomic ideal gas EOS ($\gamma = \frac{7}{5}$), are performed with CFL$= 0.5$. The first one is a left outgoing 1-rarefaction wave with the following initial condition:

$$\begin{cases} (\rho_L, u_L, P_L) = \left(1\,\mathrm{kg/m^3}, 0\,\mathrm{m/s}, 10^5\,\mathrm{Pa}\right), \\ (\rho_R, u_R, P_R) = \left(0.5\,\mathrm{kg/m^3}, 242.2\,\mathrm{m/s}, 3.789\times 10^4\,\mathrm{Pa}\right). \end{cases}$$

The second one is a right outgoing 3-shock wave with the initial condition:

$$\begin{cases} (\rho_L, u_L, P_L) = \left(1\,\mathrm{kg/m^3}, 418.3\,\mathrm{m/s}, 2.75\times 10^5\,\mathrm{Pa}\right), \\ (\rho_R, u_R, P_R) = \left(0.5\,\mathrm{kg/m^3}, 0\,\mathrm{m/s}, 10^5\,\mathrm{Pa}\right). \end{cases}$$

The numerical convergence of the scheme, when waves are gone out of the bounded computational domain $\Omega = (-200\,\mathrm{m}, 200\,\mathrm{m})$, is measured with the discrete relative L^1 norm of the error.

For smooth waves, boundary conditions BC_0 and BC_r enable to guarantee consistency when waves are going out ($t_0 < t < t_1$) or are gone out ($t > t_1$) of Ω. As expected for ideal gas EOS [7], the numerical rates of convergence for variables (u, P) are approximately 0.85, close to 1, and thus identical to those arising for $t < t_0$, see [7, 8]. The numerical errors and the rates of convergence are collected in Table 1 and Fig. 2 for an outgoing rarefaction wave, and in Table 2 and Fig. 3 when

the whole rarefaction wave has left the computational domain. BC_r condition gives very similar errors and does not provide more accurate approximations.

In contrast, BC_0 condition does not ensure the consistency of the scheme for an outgoing shock wave (at $t > t_0$, shock is outside of Ω), see Fig. 4: clearly, approximate solutions converge towards another solution when $(\Delta x, \Delta t) \to (0,0)$.

BC_s boundary condition, for a finite value of the parameter $\alpha > 0$, is still not consistent (see Fig. 5). At the limit $\alpha \to +\infty$, the asymptotic condition BC_s allows to retrieve the consistency of the approximate solution with the exact solution.

Further works aim at considering another boundary condition for outgoing shock waves based on an imposed scalar value outside and the Rankine-Hugoniot relations. The issue of the supersonic shock wave case and of the dependence on the scheme [9] are being examined. To our knowledge, this measured loss of consistency has not been pointed out before.

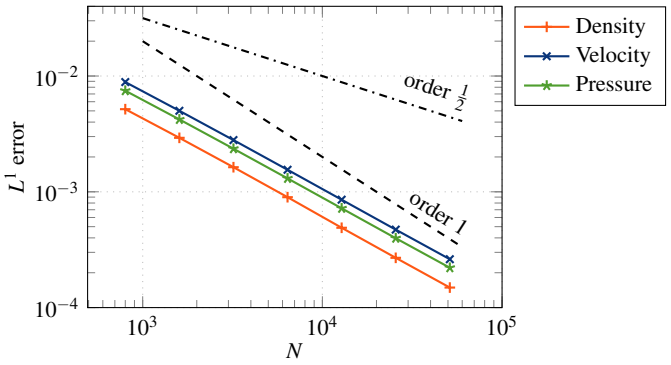

Fig. 2 BC_0: L^1 convergence curves for the rarefaction wave at $t_0 < t < t_1$.

Table 1 BC_0: L^1 convergence orders for the rarefaction wave at $t_0 < t < t_1$.

Δx (m)	N	ρ L^1 error	ρ cnv. order	u L^1 error	u cnv. order	P L^1 error	P cnv. order
5e-1	800	5.172e-3		8.868e-3		2.371e-3	
2.5e-1	1600	2.925e-3	0.8221	5.009e-3	0.8241	1.335e-3	0.8243
1.25e-1	3200	1.631e-3	0.8426	2.798e-3	0.8403	7.478e-4	0.8402
6.25e-2	6400	8.984e-4	0.8605	1.550e-3	0.8518	4.194e-4	0.8516
3.125e-2	12800	4.891e-4	0.8774	8.548e-4	0.8587	2.379e-4	0.8582
1.5625e-2	25600	2.691e-4	0.8621	4.714e-4	0.8588	1.386e-4	0.8579
7.8125e-3	51200	1.489e-4	0.8533	2.617e-4	0.8491	8.461e-5	0.8474

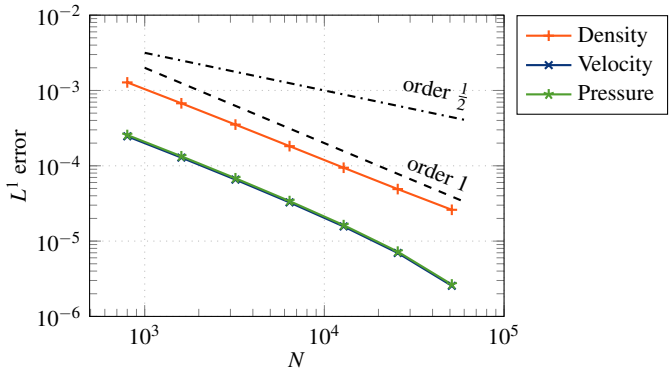

Fig. 3 BC_0: L^1 convergence curves for the rarefaction wave at $t > t_1$.

Table 2 BC_0: L^1 convergence orders for the rarefaction wave at $t > t_1$.

Δx (m)	N	ρ L^1 error	ρ cnv. order	u L^1 error	u cnv. order	P L^1 error	P cnv. order
5e-1	800	1.279e-3		2.462e-4		2.562e-4	
2.5e-1	1600	6.755e-4	0.9211	1.284e-4	0.9384	1.337e-4	0.9383
1.25e-1	3200	3.522e-4	0.9395	6.557e-5	0.9700	6.826e-5	0.9700
6.25e-2	6400	1.823e-4	0.9502	3.265e-5	1.0061	3.399e-5	1.0061
3.125e-2	12800	9.423e-5	0.9521	1.565e-5	1.0608	1.629e-5	1.0609
1.5625e-2	25600	4.904e-5	0.9420	6.962e-6	1.1687	7.247e-6	1.1687
7.8125e-3	51200	2.604e-5	0.9134	2.551e-6	1.4486	2.655e-6	1.4486

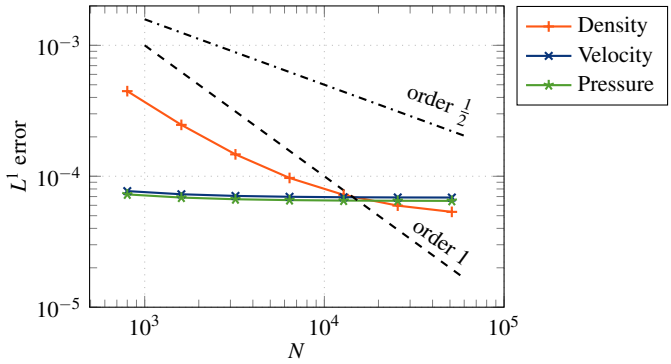

Fig. 4 BC_0: L^1 convergence curves for the shock wave at $t > t_0$.

Acknowledgements The first author received a financial support by ANRT through an EDF-CIFRE contract 2016/0728. The last author also receives a financial support by ANRT through an EDF-CIFRE contract 2017/0476. All computational facilities were provided by EDF R&D.

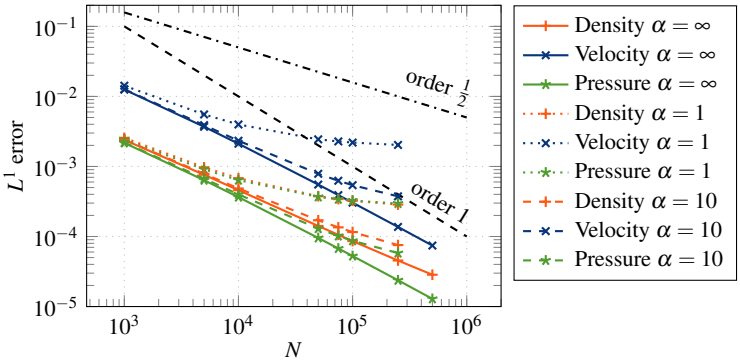

Fig. 5 BC_s: L^1 convergence curves for the shock tube at $t > t_0$.

References

1. Bardos, C., LeRoux, A.Y., Nédélec, J.C.: First order quasilinear equations with boundary conditions. Communications in Partial Differential Equations **4**(9), 1017–1034 (1979)
2. Colas, C.: Time-implicit integral formulation for fluid flow modelling in congested media. Phd thesis, Aix-Marseille Université (2019). URL https://tel.archives-ouvertes.fr/tel-02382958
3. Deininger, M., Iben, U., Munz, C.D.: Coupling of three- and one-dimensional hydraulic flow simulations. Computers & Fluids **190**, 128 – 138 (2019)
4. Dubois, F.: Boundary conditions and the Osher scheme for the Euler equations of gas dynamics. Internal Report CMAP 170, Ecole Polytechnique, Palaiseau, France (1987)
5. Dubois, F., Le Floch, P.: Boundary conditions for nonlinear hyperbolic systems of conservation laws. J. Diff Equations **71**(1), 93–122 (1988)
6. Gallouët, T.: Boundary conditions for hyperbolic equations or systems. In: M. Feistauer, V. Dolejší, P. Knobloch, K. Najzar (eds.) Numerical Mathematics and Advanced Applications, pp. 39–55. Springer Berlin Heidelberg, Berlin, Heidelberg (2004)
7. Gallouët, T., Hérard, J.M., Seguin, N.: Some recent Finite Volume schemes to compute Euler equations using real gas EOS. International Journal for Numerical Methods in Fluids **39**, 1073–1138 (2002). URL https://hal.archives-ouvertes.fr/hal-01290885
8. Gallouët, T., Hérard, J.M., Seguin, N.: On the use of symmetrizing variables for vacuum. Calcolo **40**(3), 163–194 (2003). URL https://hal.archives-ouvertes.fr/hal-00003439
9. Quibel, L.: Simulation d'écoulements diphasiques eau-vapeur avec un modèle homogène. Phd thesis in preparation, Université de Strasbourg. URL http://www.theses.fr/s188859
10. Smoller, J.: Shock Waves and Reaction-Diffusion Equations, *A Series of Comprehensive Studies in Mathematics*, vol. 258. Springer-Verlag, New York (1994)